

OPTICS  
AND LASER PHYSICS

# On the Possibility of Propagation of Gamma-Ray Photons at a Velocity Less Than 6 m/s at Room Temperature by Means of Acoustically Induced Transparency

Y. V. Radeonychev<sup>a, b, \*</sup>, I. R. Khairulin<sup>a, b</sup>, and O. A. Kocharovskaya<sup>c</sup>

<sup>a</sup> Federal Research Center Institute of Applied Physics, Russian Academy of Sciences, Nizhny Novgorod, 603950 Russia

<sup>b</sup> Lobachevsky State University of Nizhny Novgorod, Nizhny Novgorod, 603950 Russia

<sup>c</sup> Department of Physics and Astronomy and Institute for Quantum Studies and Engineering, Texas A&M University, College Station, TX 77843-4242, USA

\*e-mail: radion@appl.sci-nnov.ru

Received November 12, 2021; revised November 12, 2021; accepted November 12, 2021

In [Y.V. Radeonychev et al., Phys. Rev. Lett. **124**, 163602 (2020)], we reported the observation of the acoustically induced transparency of a stainless steel foil for 14.4-keV resonant gamma-ray photons from a <sup>57</sup>Co radioactive Mössbauer source, which is similar to electromagnetically induced transparency and Autler–Townes splitting. In this work, we show that the use of a stainless steel foil with a certain thickness that is enriched in <sup>57</sup>Fe and oscillates at the optimal frequency under the same experimental conditions can slow down a single-photon wave packet of gamma radiation with a duration of about 80 ns from the <sup>57</sup>Co source to a velocity of less than 6 m/s with a delay of about 100 ns at room temperature.

DOI: 10.1134/S0021364021240061

## 1. INTRODUCTION

Effects associated with the appearance of a spectral transparency window in the frequency range of strong resonant absorption of a medium are currently of great interest. Transparency through Autler–Townes splitting [1, 2], electromagnetically induced transparency [3–5], optomechanically induced transparency [6–8], acoustically induced transparency (AIT) [9–11], and their analogs in various quantum and classical systems [12–19], including diverse metamaterials [13, 15, 17–19], are some of the numerous methods to control resonant absorption of the medium and, thereby, the characteristics of radiation interacting with them in various spectral ranges from the microwave to hard X-ray range.

One of the effects accompanying the appearance of the spectral transparency window is a sufficiently strong frequency dependence of the dispersion of the medium, which can reduce the group velocity of radiation to several meters per second [20] and even to zero and negative values of its projection on the direction of the phase velocity with the appropriate use of the spatial dispersion [21]. New approaches to the creation of controlled delay lines in optical circuits, as well as to the processing of optical and quantum optical information, are developed on this foundation [2, 5, 8, 12, 13, 15, 18, 19, 22].

Impressive achievements in coherent infrared and visible optics, including control of the propagation velocity of optical pulses, stimulate studies of the possibility of application of developed methods in a higher frequency range of the electromagnetic spectrum where photon energies are from several to several hundred keV. The main sources of this radiation are synchrotrons, free-electron lasers, and laser plasma, which are sources of X rays, as well as radioactive Mössbauer sources (RMSs) of gamma radiation. The discussed spectral range is attractive not only fundamentally but also because of numerous existing and promising applications in various fields of science and technology.

Kiloelectronvolt radiation has advantages such as the possibility of its focusing to a nanometer scale, propagation in media opaque to optical radiation, generation in the form of a sequence of single photons, and their highly efficient detection. The mentioned photons can have a uniquely high degree of monochromaticity. For example, 14.4-keV photons emitted without recoil (Mössbauer radiation) in the radioactive decay of <sup>57</sup>Co nuclei have a spectral width of about 1 MHz and a coherence length exceeding 40 m. At the same time, the spectral lines of quantum transitions in <sup>57</sup>Fe nuclei that are resonant to the indicated radiation under the Mössbauer effect conditions even at room temperature have width of about 1 MHz, which is

approximately  $3 \times 10^{12}$  times smaller than the frequencies of transitions (the respective ratios for optical transitions of electrons in atoms usually range from  $10^9$  in gases to  $10^3$  in solids). In combination with a high concentrations of working nuclei in a solid (up to  $10^{23} \text{ cm}^{-3}$ ), this leads to a very large optical thickness at a small physical thickness of an absorber. In particular, an iron foil that consists of  $^{57}\text{Fe}$  nuclei and has a thickness of about 70 nm ensures the reduction of the intensity of 14.4-keV radiation by a factor of  $e$  at room temperature, which provides a foundation for fabrication of miniature solid elements of gamma-/X-ray quantum optics. The listed and other advantages of high-energy radiation and nuclear media stimulate the active development of gamma-/X-ray quantum optics.

One of the directions of such studies is the expansion of ideas and concepts of laser physics to the gamma-/X-ray range. At the same time, most methods of light control are inefficient or inapplicable directly for keV photons primarily because of the absence of sources of sufficiently intense coherent radiation used to change the optical properties of media in the visible and infrared ranges.

However, the properties of keV radiation and nuclear media listed above that are unique for atomic optics open new possibilities for controlling the gamma-/X-ray photon–nuclear ensemble interface. One of these possibilities is the use of the Doppler effect, which is particularly pronounced for radiation with a short wavelength. In particular, the motion of the  $^{57}\text{Fe}$  nucleus at a constant velocity of 0.17 mm/s along the propagation direction of 14.4-keV radiation detunes radiation from resonance with the quantum transition in the nucleus, shifting the frequency of its spectral line with a width of 1.13 MHz by 2 MHz. In practice, this motion is initiated by the displacement of the sample containing  $^{57}\text{Fe}$  nuclei at a constant velocity and underlies Mössbauer spectroscopy.

Another variant of the application of the Doppler effect to efficiently control the resonant interaction of gamma and X rays with nuclei of the medium is the use of coherent harmonic vibrations of nuclei along the direction of radiation with the same amplitude, which are initiated by means of the motion of the sample as a whole (piston-like vibration) at an ultrasonic frequency [9–11, 23–33]. The performed experiments showed that the variation of the amplitude, frequency, and initial phase of vibrations, as well as the detuning of the carrier frequency of radiation from the frequency of the quantum transition in nuclei, makes it possible to control the shape of the envelope of a single-photon wave packet passed through the absorber. As demonstrated in a series of recent works, depending on the listed parameters, the single-photon wave packet with the exponential envelope can either (i) be transformed to a regular sequence of almost spectrally limited short pulses with controlled duration and rep-

etition period [26] or bunches of pulses with various number of pulses in a bunch [27] or (ii) pass through the resonant absorber, hardly varying its intensity and spectral–temporal characteristics [10].

In [10], we demonstrated the effect of AIT of a two-level nuclear medium for resonant gamma rays emitted by a  $^{57}\text{Co}$  RMS, which was predicted in our previous work [9]. Similar to the optical effects of electromagnetically induced transparency and Autler–Townes splitting, the acoustic vibration of the absorber under certain conditions results in the appearance of the spectral transparency window in the range of resonant absorption of nuclei. Correspondingly, the dispersion of the medium has a sufficiently strong frequency dependence, which should lead to a decrease in the velocity of photons.

In this work, we show that the optimization of the parameters of the performed experiment [10], namely, the enrichment of the stainless steel foil in  $^{57}\text{Fe}$  nuclei, as well as the reduction of the frequency of its vibrations, will allow a decrease in the velocity of single gamma-ray photons to less than 6 m/s at room temperature.

## 2. GROUP VELOCITY OF RADIATION UNDER THE CONDITIONS OF ACOUSTICALLY INDUCED TRANSPARENCY

We consider the propagation of monochromatic radiation

$$E(t, z) = \bar{E}_\omega \exp(-i\omega t + ikz), \quad (1)$$

where  $z \leq 0$ , in an isotropic homogeneous medium with the length  $L$ , setting  $k = \omega/v_{\text{ph}}$ , where  $v_{\text{ph}}$  is the phase velocity of light in the medium at the frequency  $\omega$ . The group velocity  $v_g \equiv d\omega/dk'$  (where  $k = k' + ik''$ ) of the corresponding spectrally narrow wave packet with the central frequency  $\omega$  close to the frequency of the quantum transition in the medium  $\omega_{21}$  can be written in the form

$$v_g = \frac{v_{\text{ph}}}{1 + \frac{2\pi\omega}{1 + 4\pi\chi'_{21}(\omega)} \frac{d\chi'_{21}(\omega)}{d\omega}}. \quad (2)$$

Here,  $v_{\text{ph}} = c$ , where  $c$  is the speed of light in vacuum (all nonresonant interactions are assumed to be negligibly small), and  $\chi'_{21}(\omega)$  is the real part of the resonant susceptibility of the medium,  $\chi_{21}(\omega) = \chi'_{21}(\omega) + i\chi''_{21}(\omega)$ , which is determined by the relation between the amplitudes of the resonant polarization of the medium  $P(t, z) = \bar{P}_\omega e^{-i\omega t + ikz}$  and monochromatic field (1)  $\bar{P}_\omega = \chi_{21}(\omega)\bar{E}_\omega$ . The polarization of the medium within the two-level model can be defined as

$P = f_a N d_{12} \rho_{21}$ , where  $\rho_{21}$  is the induced resonant coherence (off-diagonal element of the density matrix) of the  $|1\rangle\text{--}|2\rangle$  quantum transition;  $f_a$  is the Lamb–Mössbauer factor, which describes the probability of recoil-free absorption of a photon by a nucleus;  $N$  is the concentration of resonant nuclei; and  $d_{12} = d_{21}^*$  is the effective dipole moment of the  $|1\rangle\text{--}|2\rangle$  resonant quantum transition [34, 35]. Coherence is determined by the equation for the density matrix of the medium; taking into account the motion of atoms in the laboratory reference frame, this equation in the case of the homogeneously broadened quantum transition has the form [9, 10, 34, 36]

$$\frac{\partial \rho_{21}}{\partial t} + \frac{\partial \rho_{21}}{\partial z} \frac{dz}{dt} + (i\omega_{21} + \gamma_{21})\rho_{21} = in_{12} \frac{d_{21} E(t, z)}{\hbar}. \quad (3)$$

Here,  $\gamma_{21}$  is the decay rate of coherence on the  $|1\rangle\text{--}|2\rangle$  transition, which determines the half-width of the absorption line of the transition;  $n_{12} \approx 1$  is the difference in population between the lower and upper levels involved in the transition;  $dz/dt$  is the velocity of nuclei along the field propagation direction; and  $\hbar$  is the reduced Planck constant.

Following [10], we consider synchronous harmonic vibrations of nuclei with the same amplitude along the resonant field propagation direction,

$$z(t) = z_a + R \sin(\Omega t + \vartheta), \quad (4)$$

where  $R$ ,  $\Omega$ , and  $\vartheta$  are the amplitude, frequency, and initial phase of vibrations, respectively, and  $z_a$  is the coordinate in the reference frame oscillating with the medium. Equation (4) implies that the thickness of the absorber  $L$  is much smaller than the wavelength of sound in the absorber,  $L \ll 2\pi V_s/\Omega$ , where  $V_s$  is the speed of sound, and its motion is nonrelativistic,  $R\Omega \ll c$ . Substituting Eq. (4) into Eq. (3), one can show that the frequency of the quantum transition in the vibrating medium in the laboratory reference frame becomes modulated [9–11, 26, 29, 30, 32, 33],  $\tilde{\omega}_{21} = \omega_{21} + kR\Omega \cos(\Omega t + \vartheta)$ . The subsequent integration of Eq. (3) with the monochromatic field (1) substituted into its right-hand side using the Jacobi–Anger relation  $e^{\pm ip \sin \phi} = \sum_{n=-\infty}^{\infty} J_n(p) e^{\pm in\phi}$ , where  $J_n(p)$  is the Bessel function of the first kind and  $p = kR$  is the index of the frequency modulation of the quantum transition, gives a solution at the leading bound of the medium  $z = 0$  in the form [9]

$$\rho_{21} = \rho_{21}^{(0)} + \sum_{q=-\infty, q \neq 0}^{\infty} \rho_{21}^{(q)}, \quad (5)$$

where

$$\rho_{21}^{(0)} = \frac{d_{21} \bar{E}_\omega}{\hbar \gamma_{21}} n_{12} e^{-i\omega t} \sum_{n=-\infty}^{\infty} \eta_n J_n^2(p), \quad (6)$$

$$\rho_{21}^{(q)} = \frac{d_{21} \bar{E}_\omega}{\hbar \gamma_{21}} n_{12} e^{-iq\vartheta - i(\omega + q\Omega)t} \sum_{n=-\infty}^{\infty} \eta_{n-q} J_{n-q}(p) J_n(p), \quad (7)$$

$$\eta_n = \frac{(\omega_{21} - \omega + n\Omega)/\gamma_{21} + i}{(\omega_{21} - \omega + n\Omega)^2/\gamma_{21}^2 + 1}. \quad (8)$$

Expressions (5)–(8) show that the resonant monochromatic field induces the polarization in the vibrating medium not only at the eigenfrequency  $\omega$  (see Eq. (6)) but also at combination frequencies  $\omega + q\Omega$ ,  $q \in \mathbb{Z}$  (see Eq. (7)). As a result, the field at combination frequencies is generated under certain conditions, and the synchronization of generated spectral components leads to the transformation of the incident monochromatic radiation to a sequence of short pulses [26, 27, 29, 30, 32, 33]. The considered case of AIT occurs under different conditions the main of which is a certain amplitude of vibrations of the absorber [9–11]:

$$R = R_i, \quad \text{where} \quad R_1 \approx 0.38\lambda, R_2 \approx 0.88\lambda, \dots, \quad (9)$$

which corresponds to the modulation index

$$p = p_i, \quad \text{where} \quad p_1 \approx 2.4, p_2 \approx 5.5, \dots \quad (10)$$

At these values,  $J_0(p_i) \approx 0$ ; i.e., resonant terms disappear in Eqs. (6) and (7). The remaining terms include a quantity multiple to  $\Omega$  in the denominator, and if the frequency of vibrations of the absorber is high enough,  $\Omega/\gamma_{21} > 1$ , the resonant-field-induced polarization of the quantum transition (proportional to coherence given by Eq. (5)) can be very small. In other words, AIT occurs in the medium.

We consider only the case  $p = p_1$ , where the susceptibility of the medium at the frequency of the field according to Eq. (6) has the form (Fig. 1)

$$\chi_{21}(\omega) = \chi_0 \sum_{n=-\infty}^{\infty} J_n^2(p_1) \eta_n, \quad (11)$$

where  $\chi_0 = f_a n_{12} |d_{21}|^2 N / (\hbar \gamma_{21})$ .

According to Eq. (11) and Fig. 1, in the case of the homogeneously broadened spectral line of the quantum transition and the frequency of vibrations of the absorber  $\Omega/\gamma_{21} = 3$ , resonant absorption in the middle of the spectral transparency window  $\omega = \omega_{21}$  decreases by a factor of 15, and the dispersion has a large slope, which determines the group velocity of the field in the medium according to (2). Taking into account Eq. (11), the group velocity can be represented in the form

$$v_g = \frac{c}{1 + 4\pi Q \chi_0 \sum_{n=-\infty}^{\infty} J_n^2(p_1) \frac{(n\Omega/\gamma_{21})^2 - 1}{[(n\Omega/\gamma_{21})^2 + 1]^2}}, \quad (12)$$

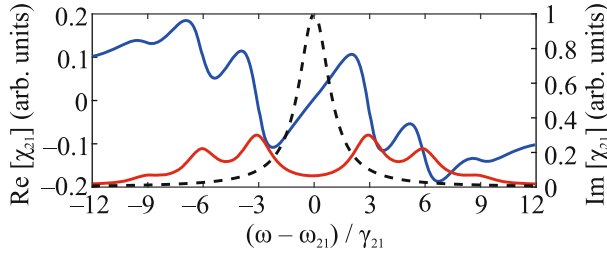


**Fig. 1.** (Color online) (Red line, right axis) Absorbance and (blue line, left axis) dispersion of the vibrating resonant absorber in the laboratory reference frame in the case of acoustically induced transparency according to Eq. (11) at  $p = p_1 = 2.4$  and  $\Omega/\gamma_{21} = 3$ . The black dashed line (right axis) is the spectral absorption line of the absorber at rest plotted according to Eq. (11) at  $p_1 = 0$ . This line is also the spectrum of the incident wave packet with the Lorentzian spectrum (20) having the half-width  $\gamma_{21}$  in the laboratory reference frame.

where  $Q = \omega_{21}/(2\gamma_{21})$  is the  $Q$ -factor of the quantum transition. Let us use Eq. (12) to estimate the group velocity of the 14.4-keV single-photon wave packet in the experiment on the observation of AIT [10] in the  $\text{Fe}_{70}\text{Cr}_{19}\text{Ni}_{11}$  stainless steel foil with the natural content of  $^{57}\text{Fe}$  nuclei ( $\approx 2\%$ ). The physical and optical thicknesses of the foil were  $L \approx 25 \mu\text{m}$  and  $T_a \approx 5.2$ , respectively; the frequency of vibrations was  $\Omega/(2\pi) \approx 9.87 \text{ MHz}$ ; and the half-width of the spectral line of the resonant quantum transition in  $^{57}\text{Fe}$  nuclei was  $\gamma_{21}/(2\pi) \approx 0.85 \text{ MHz}$ . In this case,  $Q \approx 2.1 \times 10^{12}$ ,  $\chi_0 \approx 2.3 \times 10^{-7}$ , and the sum in Eq. (12) is approximately 0.005; the substitution of these parameters into Eq. (12) gives  $v_g \approx 10^4 \text{ m/s}$ . According to Eq. (12), the group velocity can be reduced by (i) decreasing the frequency of vibrations of the foil  $\Omega$ , (ii) increasing the concentration  $N$  of  $^{57}\text{Fe}$  nuclei, (iii) increasing the Lamb–Mössbauer factor  $f_a$ , and (iv) decreasing the half-width  $\gamma_{21}$  of the spectral line of the quantum transition to the natural half-width  $\gamma_{21}/(2\pi) \approx 0.56 \text{ MHz}$ . The width of the spectral line can be reduced and the Lamb–Mössbauer factor of the absorber can be increased by changing its chemical composition and crystal structure (introducing  $^{57}\text{Fe}$  nuclei into a harder crystal matrix), as well as by reducing the temperature. In the case considered in [10], the concentration of  $^{57}\text{Fe}$  nuclei in the iron fraction can be increased to 95% according to [24, 25, 36] and even to 98% according to [37]. In the latter case, we obtain  $4\pi Q\chi_0 \approx 2.97 \times 10^8$ . The reduction of the frequency of vibrations of the foil to 2.54 MHz, which corresponds to  $\Omega/\gamma_{21} \approx 3$ , increases the sum in Eq. (12) to 0.05. As a result, the group velocity of radiation becomes  $v_g \approx 20 \text{ m/s}$ .

### 3. PROPAGATION OF 14.4-keV PHOTONS UNDER THE CONDITIONS OF ACOUSTICALLY INDUCED TRANSPARENCY

The experiment reported in [10] was performed with radiation in the form of a sequence of single 14.4-keV photons emitted by the  $^{57}\text{Co}$  RMS (Fig. 2). We measured the time interval from the detection of a 122-keV photon, i.e., the excitation of the nucleus in the RMS that emits a 14.4-keV photon (i.e., the appearance of the possibility of photon emission), to the detection of the photon and the number of photons detected after this interval in multiply repeated events of the emission and detection of the photon. As a result, the single-photon wave packet was formed with the intensity (waveform) proportional to the detection probability of the 14.4-keV photon as a function of the time from the detection of the 122-keV photon (this time instant specifies the beginning of the single-photon wave packet).

The propagation velocity of 14.4-keV gamma photons in the resonance nuclear absorber is defined as

$$v \equiv L/\Delta t_M. \quad (13)$$

Here,  $L$  is the physical thickness of the absorber and  $\Delta t_M = t_{\text{max}}^{(\text{out})} - t_{\text{max}}^{(\text{in})}$  is the time of propagation of the single-photon wave packet in the medium, where  $t_{\text{max}}^{(\text{out})}$  and  $t_{\text{max}}^{(\text{in})}$  are the time instants of the formation of intensity maxima at the output and input of the medium, respectively. The difference of the velocity of the wave packet in the medium from the velocity in free space results in the appearance of the time delay given by the expression

$$\tau_d = \Delta t_M - \Delta t_{\text{FS}}, \quad (14)$$

where  $\Delta t_{\text{FS}} = L/c$  is the time of passage of the wave packet through the distance  $L$  in free space. According to Eqs. (13) and (14), if  $v \ll c$ , it is possible to accept that  $v = L/\tau_d$  and  $\tau_d = \Delta t_M$ .

It is convenient to determine the intensity of the single-photon wave packet passed through the absorber in the reference frame of the absorber, which oscillates according to the law (4). In this reference frame, the absorber is at rest, and its resonant susceptibility is given by the well-known expression (see also [10, 36])

$$\chi_{21}^{(\text{vib})}(\omega) = \chi_0 \frac{(\omega_{21} - \omega)/\gamma_{21} + i}{(\omega_{21} - \omega)^2/\gamma_{21}^2 + 1}. \quad (15)$$

Expression (15) also follows from Eq. (11) at  $p_1 = 0$ . In this case, the incident monochromatic field becomes frequency modulated,  $E(t, z_a = 0) = \bar{E}_\omega \exp[-i\omega t + ikR \sin(\Omega t + \vartheta)]$ , which directly follows from the substitution of Eq. (4) into Eq. (1). According to the Jacobi–Anger relation, the frequency modu-

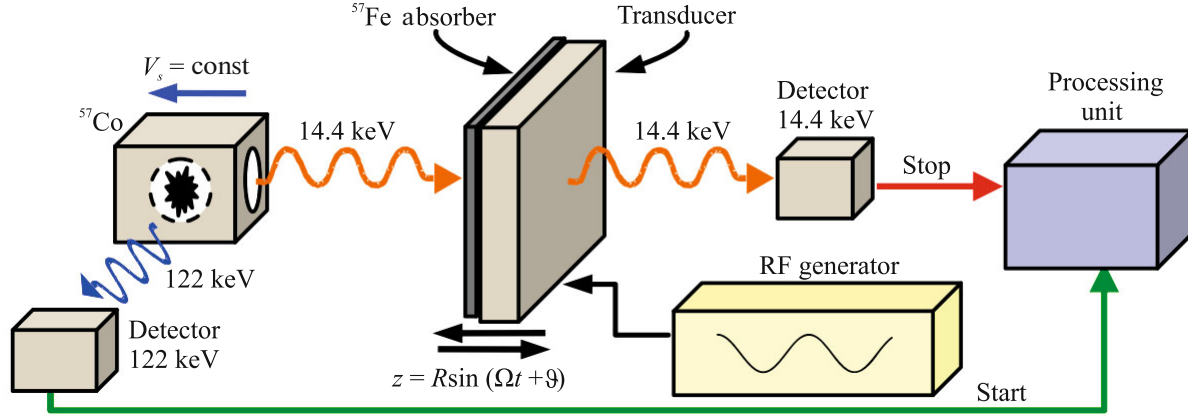


**Fig. 2.** (Color online) Scheme of the experiment [10] on the observation of acoustically induced transparency for 14.4-keV photons in the vibrating stainless steel foil. The detection of a 122-keV photon indicates the excitation of nuclei in the  $^{57}\text{Co}$  radioactive Mössbauer source, i.e., the possibility of emission of a 14.4-keV photon by the source. The multiply measured interval between the Start and Stop signals gives the count rate of 14.4-keV photons as a function of the time proportional to the intensity of a single-photon wave packet (time dependence of the detection probability or the waveform of the 14.4-keV photon). The radioactive Mössbauer source is moved at a constant velocity in order to match the resonant frequencies of the source and absorber. The Start signal can be delayed arbitrarily to cut off the Brillouin precursor (see main text).

lated field is equivalent to a set of equidistant monochromatic components:

$$\begin{aligned} E(t, z_a = 0) &= \bar{E}_\omega \sum_{n=-\infty}^{\infty} J_{-n}(p) e^{-in\vartheta} e^{-i(\omega+n\Omega)t} \\ &= \sum_{n=-\infty}^{\infty} \bar{E}_\omega^{(n)} e^{-i\omega_n t}, \end{aligned} \quad (16)$$

where  $\omega_n = \omega + n\Omega$ . It is assumed that the absorber is sufficiently thin,  $L \ll \pi c/|\omega_n - \omega_m|$  for any  $n$  and  $m$  values; in this case, the difference between the wave vectors of monochromatic components can be neglected. The propagation of each component  $\bar{E}_\omega^{(n)} = \bar{E}_\omega J_{-n}(p) e^{-in\vartheta}$  in the medium is described by the known wave equation for slowly varying amplitudes

$$c \frac{d\bar{E}_\omega^{(n)}}{dz_a} = i2\pi\omega_{21}\chi_{21}^{(\text{vib})}(\omega_n)\bar{E}_\omega^{(n)}, \quad (17)$$

where  $\omega_n \simeq \omega_{21}$  because  $\Omega \ll \omega_{21}$ . The Bouguer–Lambert–Beer law follows from Eq. (17) in the form [10, 34, 35]

$$\bar{E}_\omega^{(n)}(z_a) = \bar{E}_\omega J_{-n}(p) e^{-in\vartheta} \exp[i2\pi\omega_{21}\chi_{21}^{(\text{vib})}(\omega_n)z_a/c]. \quad (18)$$

The 14.4-keV single-photon wave packet emitted from the  $^{57}\text{Co}$  RMS without recoil is described by the function [10, 11, 26–35, 38, 39]

$$E_{\text{ph}}(t, z \leq 0) = E_0 \theta(t - z/c) e^{-i(\omega_S t - k_S z)} e^{-\gamma_S(t - z/c)}. \quad (19)$$

Here,  $\theta(x)$  is the Heaviside step function;  $\gamma_S \geq 1/(2T_S)$ , where  $T_S \approx 141$  ns is the lifetime of the excited state of the RMS;  $\omega_S$  is the central frequency of the spectral line of the RMS; and  $k_S = \omega_S/c$ . The spectrum of such

a wave packet at the input of the absorber ( $z = 0$ ),  $\bar{E}_{\text{ph}}(\omega) = \frac{1}{2\pi} \int_{-\infty}^{\infty} E_{\text{ph}}(t, 0) e^{i\omega t} d\omega$ , corresponding to the amplitude of the monochromatic wave (1) is described by the function

$$\bar{E}_{\text{ph}}(\omega) = \frac{E_0/(2\pi)}{\gamma_S + i(\omega_S - \omega)} \equiv \bar{E}_\omega. \quad (20)$$

Substituting Eq. (18) into Eq. (16) and taking into account Eq. (20), we obtain an expression for the field formed as a result of the propagation of the monochromatic radiation component from the RMS in the reference frame of the absorber. Integration over frequencies of all monochromatic components of the incident field (20) gives the expression for the total field of the single-photon wave packet from the RMS at the depth  $z_a$  of the absorber in the oscillating reference frame:

$$\begin{aligned} E_{\text{ph}}(t, z_a) &= \sum_{n=-\infty}^{\infty} J_{-n}(p) e^{-in\vartheta} \\ &\times \int_{-\infty}^{\infty} d\omega e^{-i(\omega+n\Omega)t} \bar{E}_{\text{ph}}(\omega) e^{i2\pi\omega_{21}\chi_{21}^{(\text{vib})}(\omega_n)z_a/c}. \end{aligned} \quad (21)$$

As shown in [10, 11, 26, 29, 30, 32], only the phase factor  $\exp[-ip \sin(\Omega t + \vartheta)]$  distinguishes the expression for the field inside the absorber in the laboratory reference frame from Eq. (21). Thus, the field intensity at

the output of the absorber  $I_{\text{out}}(t) = \frac{c}{8\pi} |E_{\text{ph}}(t, L)|^2$  is independent of the reference frame. The randomness of the times of the appearance of the excited nucleus in the RMS leads to the averaging of the intensity of the

single-photon wave packet with respect to the initial phase  $\vartheta$  of vibrations of the absorber. As a result, the waveform of the photon from the RMS measured at the output of the vibrating resonant absorber can be described as

$$\langle I_{\text{out}}(t) \rangle_{\vartheta} / I_0 = \sum_{n=-\infty}^{\infty} J_n^2(p) \times \left| \int_{-\infty}^{\infty} \bar{E}_{\text{ph}}(\omega) \exp \left\{ \frac{-T_a/2}{1 + i(\omega_{21} - \omega + n\Omega)/\gamma_{21}} \right\} e^{-i\omega t} d\omega \right|^2, \quad (22)$$

where  $I_0 = cE_0^2/(8\pi)$  and  $T_a = 4\pi\omega_{21}\chi_0 L/c$  is the Mössbauer thickness of the absorber. This waveform is shown in Fig. 3 for the parameters of vibrations of the absorber that are used for Fig. 1. At the input of the absorber in the experiment reported in [10], the Lorentzian spectral contour (20) (black dashed line in Fig. 1) of the single-photon wave packet (19) from the  $^{57}\text{Co}$  RMS corresponds to the waveform with a sharp front decaying exponentially at a time rate of  $1/(2\gamma_S) \approx 118$  ns (blue dashed line in Fig. 3).

The sharp front caused by long spectral wings weakly interacts with the resonant nuclear transition. Consequently, at the output of the absorber, a Brillouin precursor is formed with the FWHM about the time of formation of the polarization response of the medium  $\tau_r \approx 1/(T_a\gamma_{21})$  (about 30 ns in Fig. 3) and propagates without deceleration. The response of the medium formed through a time of about  $2\tau_r$  leads to the deceleration of the remaining part of the single-photon wave packet owing to the dispersion of the absorber in the acoustically induced spectral transparency window. For the parameters in Fig. 3, the delay with respect to the leading front, which characterizes the propagation time of the wave packet in the medium, is  $\Delta t_M \approx 100$  ns, which is a factor of 1.2 larger than the measured FWHM of the pulse (81.5 ns). According to Eq. (13), the velocity of photons corresponding to this propagation time is proportional to the physical thickness of the absorber. At the optical thickness  $T_a = 6$ , the minimum physical thickness  $L$  is reached at the maximum concentration of resonant nuclei. The  $\text{Fe}_{70}\text{Cr}_{19}\text{Ni}_{11}$  stainless steel foil [10] can be enriched in  $^{57}\text{Fe}$  to 98% [37]. Then, the waveform in Fig. 3 can be obtained at the physical thickness of the foil  $L \approx 0.54$   $\mu\text{m}$ , which corresponds to the propagation velocity  $v \approx 5.4$  m/s at room temperature according to Eq. (13).

The velocity of 14.4-keV photons emitted from the  $^{57}\text{Co}$  RMS that is calculated by Eqs. (13), (14), and (22) differs from the group velocity given by Eq. (12) because the width of the spectral line of the RMS is comparable with the spectral transparency window and Lorentzian wings expand far beyond this width (Fig. 1). As a result, inhomogeneous absorption and dispersion of the group velocity of the wave packet

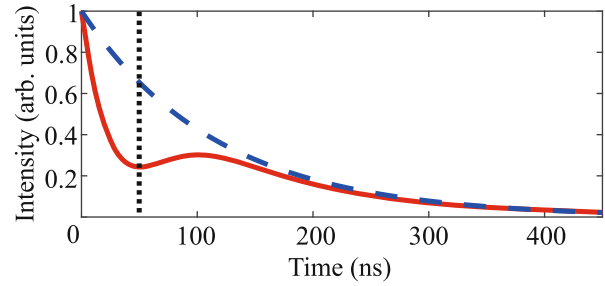


**Fig. 3.** (Color online) Time dependence of the intensity (22) of the 14.4-keV single-photon wave packet specified by Eqs. (19) and (20) that is emitted by the  $^{57}\text{Co}$  RMS with the half-width  $\gamma_S/(2\pi) = 0.68$  MHz [10] of the spectral line (blue dashed line) after the passage through the  $^{57}\text{Fe}$  absorber (red solid line) that has the half-width  $\gamma_{21}/(2\pi) = 0.85$  MHz [10] of the spectral line and the optical thickness  $T_a = 6$  and oscillates at the frequency  $\Omega/\gamma_{21} = 3$  with the amplitude  $R_1$  (see Eq. (9)) in the case  $\omega_S = \omega_{21}$ . The dotted vertical straight line marks the beginning of detection in the experiment with the cutoff of the Brillouin precursor.

occur and distort the wave packet (Fig. 3). In addition, the estimate given by Eq. (12) disregards the coherence generation described by Eq. (7) and, correspondingly, the spectral field components at the combination frequencies. Thus, the group velocity in this case is only a rough estimate of the propagation velocity of gamma-ray photons in the medium.

The presence of the Brillouin precursor in the waveform of the 14.4-keV photon masks the effect of its dispersive slowing down under the conditions of AIT, creating the impression of reshaping of the initial waveform. However, the Brillouin precursor weakly interacts with the medium. If it contains a small fraction of the energy of the wave packet (as in Fig. 3), one can expect that the delayed part of the waveform will play the main role in the subsequent processing and application of slowed-down gamma-ray photons. To directly observe the dispersive slowing down of gamma-ray photons in the vibrating absorber in the absence of the Brillouin precursor, it is sufficient to begin the detection of 14.4-keV photons (Start signal in Fig. 2) with a certain time delay after the detection of the 122-keV photon. For example, Fig. 4 shows the propagation time and velocity of 14.4-keV photons in the stainless steel foil as functions of the frequency of its vibrations and the optical thickness when the Start signal in Fig. 2 is supplied in 50 ns after the detection of the 122-keV photon (which corresponds to times to the right of the vertical black dotted straight line in Fig. 3). At the frequency of vibrations of the absorber  $\Omega/\gamma_{21} = 3$ , the maximum propagation time corresponding to the maximum dispersive delay of 14.4-keV photons,  $\Delta t_M \approx \tau_d \approx 38$  ns, is reached in the absorber with the optical thickness  $T_a \approx 5.5$  (Fig. 4a). The min-

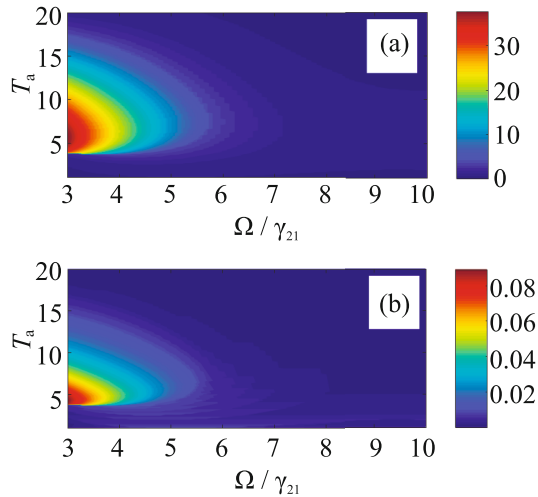


**Fig. 4.** (Color online) (a) Time instant  $\Delta t_M$  (in nanoseconds) of the formation of the maximum of the delayed 14.4-keV single-photon pulse and (b) its inverse velocity  $1/v$  (in seconds per meter) plotted according to Eqs. (13), (14), and (22) versus the dimensionless frequency of vibrations with the amplitude  $R_1$  (see Eq. (9)) at the exact resonance  $\omega_S = \omega_{21}$  and the resonant optical thickness of the absorber in the form of the  $\text{Fe}_{70}\text{Cr}_{19}\text{Ni}_{11}$  stainless steel foil [10] enriched in  $^{57}\text{Fe}$  to 98% [37]. The beginning of the detection of 14.4-keV photons (dotted vertical straight line in Fig. 3) is shifted by 50 ns from the front of the wave packet emitted by the radioactive Mössbauer source.

imum velocity of photons  $v \approx 11$  m/s in  $\text{Fe}_{70}\text{Cr}_{19}\text{Ni}_{11}$  stainless steel foil [10] enriched in  $^{57}\text{Fe}$  to 98% [37] can be reached at optical and physical thicknesses  $T_a \approx 4.2$  and  $L \approx 0.39$   $\mu\text{m}$ , respectively (Fig. 4b).

The waveform of the maximally delayed 14.4-keV photon is shown in Fig. 5. The delayed wave packet (red solid line in Fig. 5) is elongated because of the absorption of the field at the bounds of the transparency window and the dispersion of the group velocity. The comparison of Figs. 3 and 5 shows that the delay of the Lorentzian photon in the medium with AIT with respect to the sharp leading front can be approximately estimated as the sum of time intervals caused by the gradual formation of the nuclear response to the rapidly appearing action of the field of the incident wave packet and the subsequent dispersive slowing down of the photon.

Estimates obtained for the delay and velocity of 14.4-keV photons can be corrected to experimental conditions, as well as to requirements on the delay time, propagation velocity, output intensity, and the shape of the envelope of the slowed single-photon wave packet. In particular, a decrease in the frequency of vibrations of the foil increases the delay time (see Fig. 1) but simultaneously reduces the output intensity and distorts the envelope of the single-photon wave packet because a more significant part of the field spectrum is beyond the transparency window. The

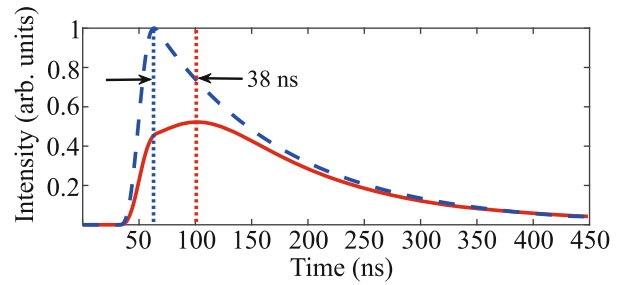


**Fig. 5.** (Color online) 50-ns delayed detection of the waveform of the 14.4-keV photon from the  $^{57}\text{Co}$  radioactive Mössbauer source with the half-width  $\gamma_S/(2\pi) = 0.68$  MHz [10] of the spectral line (blue dashed line) after the passage through the  $^{57}\text{Fe}$  absorber (red solid line) that has the half-width  $\gamma_{21}/(2\pi) = 0.85$  MHz [10] of the spectral line and the optical thickness  $T_a = 5.5$  and oscillates at the frequency  $\Omega/\gamma_{21} = 3$  with the amplitude  $R_1 = 0.38\lambda$  (see Eq. (9)) in the case  $\omega_S = \omega_{21}$ .

cutoff of the Brillouin precursor can also be implemented by different methods.

#### 4. CONCLUSIONS

To summarize, we have theoretically demonstrated the possibility of slowing down single 14.4-keV gamma-ray photons emitted by the  $^{57}\text{Co}$  radioactive Mössbauer source to 5.4 m/s in the stainless steel foil enriched in  $^{57}\text{Fe}$  at room temperature by means of acoustically induced transparency under experimental conditions implemented in [10]. Stronger deceleration can be achieved by reducing the frequency of acoustic vibrations of the foil and its temperature, as well as by changing the chemical composition of the doped matrix.

#### FUNDING

This work was supported by the Ministry of Science and Higher Education of the Russian Federation, contract no. 075-15-2020-906 with the Center of Excellence “Center of Photonics.” O.A. Kocharovskaya acknowledges the support of the US National Science Foundation, grant no. PHY-201-2194.

#### CONFLICT OF INTEREST

The authors declare that they have no conflicts of interest.

#### REFERENCES

1. S. H. Autler and C. H. Townes, Phys. Rev. **100**, 703 (1955).
2. E. Saglamyurek, T. Hrushevskiy, A. Rastogi, K. Heshami, and L. J. LeBlanc, Nat. Photon. **12**, 774 (2018).
3. O. Kocharovskaya and Ya. I. Khanin, Sov. Phys. JETP **63**, 945 (1986).

4. K. J. Boller, A. İmamođlu, and S. E. Harris, *Phys. Rev. Lett.* **66**, 2593 (1991).
5. A. Rastogi, E. Saglamyurek, T. Hrushevskiy, S. Hubele, and L. J. LeBlanc, *Phys. Rev. A* **100**, 012314 (2019).
6. S. Weis, R. Riviere, S. Deleglise, E. Gavartin, O. Arcizet, A. Schliesser, and T. J. Kippenberg, *Science* (Washington, DC, U. S.) **330**, 1520 (2010).
7. A. H. Safavi-Naeini, T. P. Mayer Alegre, J. Chan, M. Eichenfield, M. Winger, Q. Lin, J. T. Hill, D. E. Chang, and O. Painter, *Nature* (London, U.K.) **472**, 69 (2011).
8. H. Xiong and Y. Wu, *Appl. Phys. Rev.* **5**, 031305 (2018).
9. Y. V. Radeonychev, M. D. Tokman, A. G. Litvak, and O. Kocharovskaya, *Phys. Rev. Lett.* **96**, 093602 (2006).
10. Y. V. Radeonychev, I. R. Khairulin, F. G. Vagizov, M. Scully, and O. Kocharovskaya, *Phys. Rev. Lett.* **124**, 163602 (2020).
11. I. R. Khairulin, Y. V. Radeonychev, V. A. Antonov, and O. Kocharovskaya, *Sci. Rep.* **11**, 7930 (2021).
12. M. F. Yanik, W. Suh, Z. Wang, and S. Fan, *Phys. Rev. Lett.* **93**, 233903 (2004).
13. S. Zhang, D. Genov, Y. Wang, M. Liu, and X. Zang, *Phys. Rev. Lett.* **101**, 047401 (2008).
14. A. G. Litvak and M. D. Tokman, *Phys. Rev. Lett.* **88**, 095003 (2002).
15. K. Totsuka, N. Kobayashi, and M. Tomita, *Phys. Rev. Lett.* **98**, 213904 (2007).
16. R. Coussement, Y. Rostovtsev, J. Odeurs, G. Neyens, H. Muramatsu, S. Gheysen, R. Callens, K. Vyvey, G. Kozyreff, P. Mandel, R. Shakhmuratov, and O. Kocharovskaya, *Phys. Rev. Lett.* **89**, 107601 (2002).
17. R. Röhlsberger, H.-C. Wille, K. Schlage, and B. Sahoo, *Nature* (London, U.K.) **482**, 199 (2012).
18. T. Wang, Y.-Q. Hu, C.-G. Du, and G.-L. Long, *Opt. Express* **27**, 7344 (2019).
19. R. Y. M. Manjappa, Y. K. Srivastava, and R. Singh, *Appl. Phys. Lett.* **111**, 021101 (2017).
20. L. V. Hau, S. E. Harris, Z. Dutton, and C. H. Behroozi, *Nature* (London, U.K.) **397**, 594 (1999).
21. O. Kocharovskaya, Y. Rostovtsev, and M. O. Scully, *Phys. Rev. Lett.* **86**, 628 (2001).
22. Y. Okawachi, M. A. Foster, J. E. Sharping, A. L. Gaeta, Q. Xu, and M. Lipson, *Opt. Express* **14**, 2317 (2006).
23. A. R. Mkrtchyan, G. A. Arutyunyan, A. R. Arakelyan, and R. G. Gabrielyan, *Phys. Status Solidi* **92**, 23 (1979).
24. G. V. Smirnov, U. van Burck, J. Arthur, S. L. Popov, A. Q. R. Baron, A. I. Chumakov, S. L. Ruby, W. Potzel, and G. S. Brown, *Phys. Rev. Lett.* **77**, 183 (1996).
25. G. V. Smirnov and W. Potzel, *Hyperfine Interact.* **123**, 633 (1999).
26. F. Vagizov, V. Antonov, Y. V. Radeonychev, R. N. Shakhmuratov, and O. Kocharovskaya, *Nature* (London, U.K.) **508**, 80 (2014).
27. R. N. Shakhmuratov, F. G. Vagizov, V. A. Antonov, Y. V. Radeonychev, M. O. Scully, and O. Kocharovskaya, *Phys. Rev. A* **92**, 023836 (2015).
28. R. N. Shakhmuratov and F. G. Vagizov, *Phys. Rev. B* **95**, 245429 (2017).
29. Y. V. Radeonychev, V. A. Antonov, F. G. Vagizov, R. N. Shakhmuratov, and O. Kocharovskaya, *Phys. Rev. A* **92**, 043808 (2015).
30. V. A. Antonov, Y. V. Radeonychev, and O. Kocharovskaya, *Phys. Rev. A* **92**, 023841 (2015).
31. E. K. Sadykov, A. A. Yurichuk, F. G. Vagizov, Sh. I. Mubarakshin, and A. A. Valiullin, *Hyperfine Interact.* **238**, 85 (2017).
32. I. R. Khairulin, V. A. Antonov, Y. V. Radeonychev, and O. Kocharovskaya, *Phys. Rev. A* **98**, 043860 (2018).
33. I. R. Khairulin, V. A. Antonov, Y. V. Radeonychev, and O. Kocharovskaya, *J. Phys. B: At. Mol. Opt. Phys.* **51**, 235601 (2018).
34. E. Ikonen, P. Heliö, T. Katila, and K. Riski, *Phys. Rev. A* **32**, 2298 (1985).
35. Yu. V. Shvyd'ko and G. V. Smirnov, *J. Phys.: Condens. Matter* **4**, 2663 (1992).
36. S. G. Rautian, G. I. Smirnov, and A. M. Shalagin, *Nonlinear Resonances in the Spectra of Atoms and Molecules* (Nauka, Novosibirsk, 1979) [in Russian].
37. A. A. Kiselev and A. A. Opalenko, *Moscow Univ. Phys. Bull.* **40**, 106 (1985).
38. F. J. Lynch, R. E. Holland, and M. Hamermesh, *Phys. Rev.* **120**, 513 (1960).
39. G. V. Smirnov, *Hyperfine Interact.* **123–124**, 31 (1999).

*Translated by R. Tyapaev*